

# Theoretical Investigation on the Electronic Structure of Pentacyano(L)ferrate(II) Complexes with NO<sup>+</sup>, NO, and NO<sup>-</sup> Ligands. Redox Interconversion, Protonation, and Cyanide-Releasing Reactions

Mariano C. González Lebrero,<sup>†</sup> Damián A. Scherlis,<sup>†</sup> Guillermina L. Estiú,<sup>\*,†,‡</sup> José A. Olabe,<sup>\*,†</sup> and Darío A. Estrin<sup>\*,†</sup>

Departamento de Química Inorgánica, Analítica y Química Física, Inquimae, Facultad de Ciencias Exactas y Naturales, Universidad de Buenos Aires, Pabellón 2, Ciudad Universitaria, C1428EHA Buenos Aires, República Argentina, and Cequinor, Departamento de Química, Facultad de Ciencias Exactas, Universidad Nacional de La Plata, CC 962, La Plata, República Argentina

Received February 1, 2001

Reaction pathways for the one- and two-electron reductions of [Fe(CN)<sub>5</sub>NO]<sup>2-</sup> have been investigated by means of a density functional theory (DFT) approach combined with the polarized continuum model (PCM) of solvation. In addition, UV–vis spectroscopic data were obtained using ZINDO/S calculations including a point-charge model simulation of solvent effects. DFT methodologies have been used to assess the thermodynamical feasibility of protonation and cyanide-release processes for the reduced species. We conclude that [Fe(CN)<sub>5</sub>NO]<sup>3-</sup> is a stable species in aqueous solution but may release cyanide yielding [Fe(CN)<sub>4</sub>NO]<sup>2-</sup>, consistent with experimental results. On the other hand, the [Fe(CN)<sub>5</sub>NO]<sup>4-</sup> complex turns out to be unstable in solution, yielding the product of cyanide release, [Fe(CN)<sub>4</sub>NO]<sup>3-</sup>, and/or the protonated HNO complex. All the structural and spectroscopic (IR, UV–vis) predictions for the [Fe(CN)<sub>5</sub>HNO]<sup>3-</sup> ion are consistent with the scarce but significant experimental evidence of its presence as an intermediate in nitrogen redox interconversion chemistry. Our computed data support an Fe<sup>II</sup>(LS) + NO<sup>+</sup> assignment for [Fe(CN)<sub>5</sub>NO]<sup>2-</sup>, an Fe<sup>II</sup>(LS) + NO assignment for the one-electron reduction product, but an Fe<sup>I</sup>(LS) + NO<sup>+</sup> for the one-electron product after dissociation of an axial cyanide, and an Fe<sup>II</sup> + singlet NO<sup>-</sup> for the two-electron reduction species.

## Introduction

The chemistry of transition-metal nitrosyl complexes has been of great interest during past decades.<sup>1</sup> This interest has increased in recent years as the importance of nitric oxide in a variety of physiological processes has been realized.<sup>2</sup> In addition to its coordination ability toward metal centers (dissociation and formation reactions), the redox interconversion of bound NO into its oxidized (NO<sup>+</sup>) or reduced (NO<sup>-</sup>) species has attracted the attention of modern coordination chemists, due to its relation to relevant biological functions.<sup>3</sup> Although the focus of the latter studies is placed in the chemistry of NO complexes with porphyrin-like coligands,<sup>4</sup> interest in classical coordination chemistry remains alive, with emphasis in disclosing the different factors influencing NO reactivity, e.g., by changing the metals, coligands, and the medium.<sup>5</sup>

A mechanism proposed for the in vivo action of NO by using transition-metal complexes is associated with the reduction of

the formally named NO<sup>+</sup> species to NO. The subsequent dissociation of the Fe–NO bond and release of NO to the medium is followed by further activation of several different processes.<sup>2</sup> On the other hand, the more reduced form, NO<sup>-</sup> (or its protonated form, HNO), has been suggested to play an important role in many biological systems. Multiple evidences exist of it as being an intermediate either in the biosynthesis of NO mediated by the NO-synthase enzyme or in the redox interconversions of nitrogenated species in natural cycles.<sup>2</sup> Recently, the HNO adduct of myoglobin has been prepared and characterized in aqueous solution.<sup>4d</sup> The so-called “nitroxyl” species are precursors of the formation of N<sub>2</sub>O or of peroxy-nitrite species upon reaction with dioxygen.<sup>2</sup> It has been also suggested that NO<sup>-</sup> should be a necessary intermediate in the multielectronic reduction of NO<sup>+</sup> down to hydroxylamine or ammonia carried out by several coordination compounds containing low-spin d<sup>6</sup> metal centers (Fe, Ru).<sup>6,7</sup>

Coordination compounds containing nitrosyl species in any of the three redox forms have been documented.<sup>1,2</sup> However, it

\* To whom correspondence should be addressed. Fax: 54-11-4576-3341. E-mail: dario@q1.fcen.uba.ar.

<sup>†</sup> Universidad de Buenos Aires.

<sup>‡</sup> Universidad Nacional de La Plata.

- (1) (a) Richter-Addo G. B.; Legzdins P. *Metal Nitrosyls*; Oxford University Press: New York, 1992. (b) Westcott, B. L.; Enemark, J. H. In *Inorganic Electronic Structure and Spectroscopy, Volume II: Applications and Case Studies*; Solomon, E. I., Lever, A. B. P., Eds.; Wiley: New York, 1999. (c) McCleverty, J. A. *Chem. Rev.* **1979**, *79*, 53. (d) Eisenberg, R.; Meyer, C. D. *Acc. Chem. Res.* **1975**, *8*, 26.
- (2) (a) Feelisch M., Stamler, J. S., Eds. *Methods in Nitric Oxide Research*; J. Wiley & Sons: Chichester, 1996. (b) Clarke, M. J.; Gaul, J. B. *Struct. Bonding (Berlin)* **1993**, *81*, 147. (c) Butler, A. R.; Williams, L. H. *Chem. Soc. Rev.* **1993**, 233.
- (3) Stamler, J. S.; Singel, D. J.; Loscalzo, J. *Science* **1992**, *258*, 1898.

- (4) (a) Bohle, D. S.; Hung, D. H. *J. Am. Chem. Soc.* **1995**, *117*, 9584. (b) Laverman, L. E.; Hoshino, M.; Ford, P. C. *J. Am. Chem. Soc.* **1997**, *119*, 12663. (c) Ding, X. D.; Weischel, A.; Andersen, J. F.; Shokireva, T. K.; Balfour, C.; Pierik, A. J.; Averill, B. A.; Montfort, W. R.; Walker, F. A. *J. Am. Chem. Soc.* **1999**, *121*, 128. (d) Lin, R.; Farmer, P. J. *J. Am. Chem. Soc.* **2000**, *122*, 2393 and references therein. (e) Scherlis, D. A.; Cymmerlyng, C.; Estrin, D. A. *Inorg. Chem.* **2000**, *39*, 2352.
- (5) (a) Baraldo, L. M.; Bessega, M. S.; Rigotti, G. E.; Olabe, J. A. *Inorg. Chem.* **1994**, *33*, 5890. (b) Olabe, J. A.; Gentil, L. A.; Rigotti, G. E.; Navaza, A. *Inorg. Chem.* **1984**, *23*, 4297. (c) Forlano, P.; Parise, A. R.; Olabe, J. A. *Inorg. Chem.* **1998**, *37*, 6406.

was previously unprecedented to find adequate metal–coligand fragments allowing the interconversion of all these forms in a controlled way without dissociation, as recently reported for a series of complexes derived from the  $[\text{Ru}^{\text{II}}(\text{hedta})]^-$  fragment (hedta = *N*-(hydroxyethyl)ethylenediaminetriacetate).<sup>8</sup> The complexes with low-spin  $d^6$  configurations are good potential candidates for this situation. Therefore, it seems worthy to focus the research effort on the pentacyanonitrosylferrate(II) ion (nitroprusside), one of the oldest known nitrosyl compounds,<sup>9,10</sup> which, acting as a vasodilator, is useful in lowering blood pressure. The  $[\text{Fe}(\text{CN})_5\text{NO}]^{2-}$  ion is a well-characterized species,<sup>9</sup> and the same could be said of the one-electron reduction product,  $[\text{Fe}(\text{CN})_5\text{NO}]^{3-}$ , for which some spectroscopic information but no crystal structure is available.<sup>1,2</sup> More uncertainties exist on the electronic structure of the two-electron reduction product. Some spectroelectrochemical results<sup>7</sup> suggest that a  $\text{NO}^-$ -bound species is formed at sufficiently negative potentials upon reduction of nitroprusside, but the characterization still remains obscure.

In the present work, we search on the stability of the different redox-active species of NO bound to the pentacyano fragment by using theoretical methods. We also address on the thermodynamical feasibility of some reactions, namely protonation (either of the cyanides or nitrosyl moieties) and cyanide-dissociation reactions, which are relevant to the chemistry of these species. A density functional theory (DFT) scheme combined with the polarized continuum model (PCM) for taking into account solvent effects has been used for the calculations. In addition, the IR and UV spectra of the stable species were computed using DFT and ZINDO/S techniques, respectively. The predictions have been finally compared with all the available structural and spectroscopic information.

## Methods

The DFT calculations were performed by using a Gaussian basis set scheme, as implemented in the program DFT-Molecole.<sup>11</sup> The Kohn–Sham self-consistent procedure was applied to obtain the electronic density and energy through the determination of a set of one-electron orbitals.<sup>12</sup> Gaussian basis sets were used for the expansion of the one-electron orbitals and also for the additional auxiliary set used for expanding the electronic density. Matrix elements of the exchange–correlation potential were calculated by a numerical integration scheme.<sup>13</sup> The orbital and auxiliary basis sets optimized by Sim et al.<sup>14</sup> for DFT calculations were used for C, N, and H atoms. Basis sets for Fe were taken from ref 15. The contraction patterns were (5211/411/1) for C and N, (4333/431/41) for Fe, and (41/1) for H. The contraction patterns for the electronic density expansion sets were as follows: (111111/111/1) for C and N, (111111111/111/111) for Fe,

and (111111/1) for H.<sup>16</sup> A more detailed description of the technical aspects of the program is given in ref 11. Geometries were optimized for the isolated systems within the local density approximation (LDA) using the Vosko–Wilk–Nusair correlation functional.<sup>17</sup> It has been shown that LDA performs well in predicting bond distances and angles in Werner-type transition-metal complexes.<sup>18,19</sup> Single-point calculations were performed at the LDA gas-phase optimized geometries using the GGA Becke and Perdew combination of functionals for exchange and correlation, respectively.<sup>20,21</sup> The GGA level of theory has been found to be necessary to obtain reliable metal–ligand bond dissociation energies. Specifically, in the case of Fe and Ru complexes, it has been shown that good agreement with gas-phase measurements is achieved at the GGA level for metal carbonyls.<sup>22</sup> Normal modes were computed at the LDA level for the isolated systems by numerical differentiation of analytical energy gradients. Free energies at 298 K were estimated by adding thermal corrections to take into account the change in population of vibrational, rotational and translational levels, and the entropic contributions to the computed electronic energy.<sup>23</sup> Solvent effects were modeled using the polarized continuum model (PCM) scheme, in which the self-consistency between the solute wave function and solvent polarization is achieved during the self-consistent field cycle.<sup>24</sup> All PCM computations were performed using the GAUSSIAN 98 software package at the gas-phase optimized geometries.<sup>25</sup>

Electronic spectra were computed by means of the ZINDO/S methodology, included in the ZINDO program package.<sup>26</sup> This model has been extensively used for electronic spectroscopy<sup>27</sup> and its performance widely demonstrated. A review of the underlying model Hamiltonian has been furnished in ref 28. The model is based on the original INDO of Pople, Santry, and Segal<sup>29,30</sup> and is similar to the complete neglect of differential overlap (CNDO) adopted for spectroscopy by DelBene and Jaffe.<sup>31,32</sup> The CNDO model, however, does not contain the one-center two-electron terms (Slater–Condon factors)<sup>33</sup> and, therefore, is not suitable for excited states of transition-metal

- (6) (a) Armor, J. *Inorg. Chem.* **1973**, *12*, 1959. (b) Barley, M. H.; Takeuchi, K. J.; Meyer, T. J. *J. Am. Chem. Soc.* **1986**, *108*, 5876. (c) Murphy, W. R.; Takeuchi, K.; Barley, M.; Meyer, T. J. *Inorg. Chem.* **1986**, *25*, 1041. (d) Barley, M. H.; Rhodes, M. R.; Meyer, T. J. *Inorg. Chem.* **1987**, *26*, 1746. (e) Rhodes, M. R.; Barley, M. H.; Meyer, T. J. *Inorg. Chem.* **1991**, *30*, 629.
- (7) Masek, J.; Maslova, E. *Collect. Czech. Chem. Commun.* **1974**, *39*, 2141.
- (8) Chen, Y.; Lin, F. T.; Shepherd, R. E. *Inorg. Chem.* **1999**, *38*, 973.
- (9) Swinehart, J. H. *Coord. Chem. Rev.* **1967**, *2*, 385.
- (10) Butler, A. H.; Glidewell, C. *Chem. Soc. Rev.* **1987**, *16*, 361.
- (11) Estrin, D. A.; Corongiu, G.; Clementi, E. In *METECC, Methods and Techniques in Computational Chemistry*; Clementi, E., Ed.; Stef: Cagliari, 1993; Chapter 12.
- (12) Kohn, W.; Sham, L. J. *J. Phys. Rev.* **1965**, *A140*, 1133.
- (13) Becke, A. D. *J. Chem. Phys.* **1988**, *88*, 1053.
- (14) (a) Sim, F.; Salahub, D. R.; Chin, S.; Dupuis, M. *J. Chem. Phys.* **1991**, *95*, 4317. (b) Sim, F.; St-Amant, A.; Papai, Y.; Salahub, D. R. *J. Am. Chem. Soc.* **1992**, *114*, 4391.
- (15) Andzelm, J.; Radzio, E.; Salahub, D. R. *J. Comput. Chem.* **1985**, *6*, 520.

- (16) Godbout, N.; Salahub, D.; Andzelm, J.; Wimmer, E. *Can. J. Chem.* **1992**, *70*, 560.
- (17) Vosko, S. H.; Wilk, L.; Nusair, M. *Can. J. Chem.* **1980**, *58*, 1200.
- (18) Bray, M. R.; Deeth, R. J.; Paget, V. J.; Sheen, P. D. *Int. J. Quantum Chem.* **1996**, *61*, 85.
- (19) Sosa, C.; Andzelm, J.; Elkin, B. C.; Wimmer, E. *J. Phys. Chem.* **1992**, *96*, 6630.
- (20) Perdew, P. W. *Phys. Rev.* **1986**, *B33*, 8800; Erratum, *B34*, 7406.
- (21) Becke, A. D. *Phys. Rev.* **1988**, *A38*, 3098.
- (22) Li, J.; Schreckenbach, G.; Ziegler, T. *J. Am. Chem. Soc.* **1995**, *117*, 486.
- (23) Hill, T. L. *An Introduction to Statistical Thermodynamics*; Dover Publications: New York, 1986.
- (24) Cossi, M.; Barone, V.; Cammi, R.; Tomasi, J. *Chem. Phys. Lett.* **1996**, *255*, 327.
- (25) Frisch, M. J.; Trucks, G. W.; Schlegel, H. B.; Scuseria, G. E.; Robb, M. A.; Cheeseman, J. R.; Zakrzewski, V. G.; Montgomery, J. A., Jr.; Stratmann, R.; Burant, J.; Dapprich, S.; Millam, J. M.; Daniels, A. D.; Kudin, K. N.; Strain, M. C.; Farkas, O.; Tomasi, J.; Barone, V.; Cossi, M.; Cammi, R.; Mennucci, B.; Pomelli, C.; Adamo, C.; Clifford, S.; Ochterski, J.; Petersson, G. A.; Ayala, P. Y.; Cui, Q.; Morokuma, K.; Malick, D. K.; Rabuck, A. D.; Raghavachari, K.; Foresman, J. B.; Cioslowski, J.; Ortiz, J. V.; Baboul, A. G.; Stefanov, B. B.; Liu, G.; Liashenko, A.; Piskorz, P.; Komaromi, I.; Gomperts, R.; Martin, R. L.; Fox, D. J.; Keith, T.; Al-Laham, M. A.; Peng, C. Y.; Nanayakkara, A.; Gonzalez, C.; Challacombe, M.; Gill, P. M. W.; Johnson, B.; Chen, W.; Wong, M. W.; Andres, J. L.; Gonzalez, C.; Head-Gordon, M.; Replogle, E. S.; Pople, J. A. *Gaussian 98, Rev. A7*; Gaussian, Inc., Pittsburgh, PA, 1998.
- (26) Zerner, M. C. et al. *ZINDO Quantum Theory Project*; University of Florida, Gainesville, FL, 32611.
- (27) (a) Ridley, J.; Zerner, M. C. *Theor. Chim. Acta* **1973**, *32*, 111. (b) Estiú, G. L.; Zerner, M. C. *J. Am. Chem. Soc.* **1999**, *121*, 1893. (c) Estiú, G. L.; Rosch, N.; Zerner, M. C. *J. Phys. Chem.* **1995**, *99*, 13819. (d) Loew, G.; Harris, D. *Chem. Rev.* **2000**, *100*, 407.
- (28) Zerner, M. C. In *Reviews in Computational Chemistry*; Lipkowitz K. D., Boyd D. B., Eds.; VCH Publishing: New York, 1991.
- (29) Pople, J.; Beveridge, D.; Dobash, P. J. *J. Chem. Phys.* **1967**, *47*, 2026.
- (30) Pople, J.; Santry, D.; Segal, G. *J. Chem. Phys.* **1965**, *43*, 5129.
- (31) DelBene, J.; Jaffe, H. H. *J. Chem. Phys.* **1968**, *48*, 1807.
- (32) DelBene, J.; Jaffe, H. H. *J. Chem. Phys.* **1968**, *48*, 4050.
- (33) Slater, J. C. *Quantum Theory of Atomic Structure*; McGraw-Hill: New York, 1960.

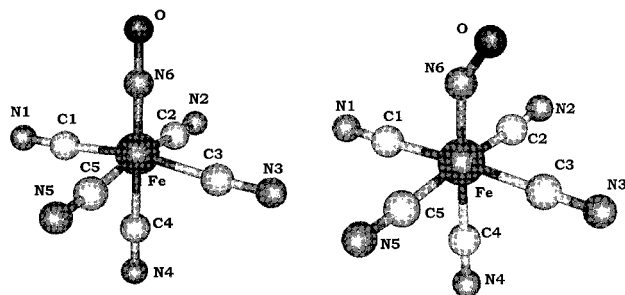


**Figure 1.** Optimized structures of  $[\text{Fe}(\text{CN})_5\text{NO}]^{2-}$  and  $[\text{Fe}(\text{CN})_5\text{NO}]^{3-}$  ions.

complexes. Most parameters of the theory come directly from atomic spectroscopy and are based on experimental ionization potentials, electron affinities, and the Slater–Condon two-electron integrals. The resonance integrals are determined empirically from a database of molecules with well-established structures and optical properties. The SCF calculations for the ground state were followed by a multireference configuration interaction (MRCI) treatment, using a Rumer diagram technique,<sup>34</sup> which is adequate for open shell structures. The structures have been derived from the DFT geometry optimizations with no further symmetrization. Oscillator strengths were evaluated with the dipole-length operator, retaining all one-center terms.

It has been already demonstrated<sup>35</sup> that the accurate interpretation of the absorption spectra of transition-metal (TM) complexes in aqueous solution requires the consideration of specific second-sphere coordination effects. For  $\text{NH}_3$ -containing complexes, Stavrev, Zerner, and Meyer showed that the positions of the metal-to-ligand charge-transfer (MLCT) excitations are successfully reproduced when a point-charge model mimics the effect of the solvent.<sup>36</sup> Following their experience, we have chosen to model point charges along the axis behind the cyanide ligands. The charge magnitudes have been adjusted in the different coordination compounds, to attain systems that are defined neutral as a whole. The particular modeling conditions are reported, for each case, in the next section. The model thus defined represents a mutually dependent solvent–ligand effect that generates an environment immediate to the complex that, together with the molecule itself, has no associated charge. Due to the large localization of the charge on the cyanide ligands, the effect of the solvent is strong and not compatible with a simulation concerning only the definition of a small number of coordinated solvent molecules. We have tested the effect of the consideration of five or 10 solvent molecules (one or two for each ligand) and found no significant change of the calculated excitation energies, although it has a sizable effect when  $\text{NH}_3$ , instead of  $\text{CN}^-$ , are the ligands.<sup>36</sup> The number of water molecules that should be included in order to attain a shift of the electronic excitations showing agreement with experiment is large enough to challenge any quantum chemical calculation. We consider this topic out of the scope of the present research, which is centered in the interpretation of experimental data.

ZINDO/S calculations are not only useful for the assignment of the UV–vis transitions but also provide further confirmation of the structural characteristics of the molecules that generate the spectra, allowing even to discern between different possible structures on the basis of the accurate reproduction of the experimental features.<sup>37</sup> The applicability of this methodology to TM complexes is based on the sensitivity of ligand field (LF) and charge-transfer (CT) transitions to structural modifications.

## Results and Discussion

**Structural and Electronic Description of  $[\text{Fe}(\text{CN})_5\text{NO}]^{n-}$  ( $n = 2-4$ ).** Figure 1 shows the geometries, optimized in a

**Table 1.** Selected Structural Parameters (Å and deg) for the  $[\text{Fe}(\text{CN})_5\text{NO}]^{n-}$  Ions ( $n = 2, 3$ ) Derived from DFT Calculations<sup>a</sup>

	$n = 2$ (exptl) <sup>b</sup>	$n = 2$	$n = 3$
$r(\text{FeC1})$	1.9403(6)	1.900	1.908
$r(\text{FeC2})$	1.9310(6)	1.896	1.913
$r(\text{FeC3})$	1.9310(6)	1.896	1.909
$r(\text{FeC4})$	1.9257(9)	1.900	1.914
$r(\text{FeC5})$	1.9403(6)	1.904	1.901
$r(\text{FeN6})$	1.6656(7)	1.621	1.737
$r(\text{C1N1})$	1.1622(8)	1.174	1.185
$r(\text{C2N2})$	1.1603(8)	1.172	1.183
$r(\text{C3N3})$	1.1603(8)	1.172	1.181
$r(\text{C4N4})$	1.1591(12)	1.174	1.182
$r(\text{C5N5})$	1.1622(8)	1.175	1.183
$r(\text{N6O})$	1.1331(10)	1.162	1.199
$\angle(\text{FeN6O})$	176.03(7)	177.2	146.6

<sup>a</sup> Experimental values are given for comparison. <sup>b</sup> Reference 38. Values in parentheses are standard deviations.

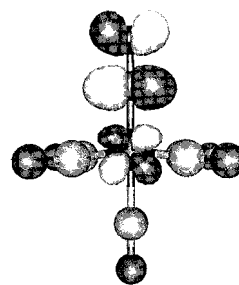


**Figure 2.** DFT computed LUMO of  $[\text{Fe}(\text{CN})_5\text{NO}]^{2-}$ .

vacuum without symmetry constraints, for the complexes with  $n = 2, 3$ . Table 1 shows the calculated bond lengths and angles, together with experimental data available for  $\text{Na}_2[\text{Fe}(\text{CN})_5\text{NO}] \cdot 2\text{H}_2\text{O}$ .<sup>38</sup> The overall agreement for the  $[\text{Fe}(\text{CN})_5\text{NO}]^{2-}$  ion is reasonable, mainly based on the consideration that LDA calculations tend to underestimate slightly the metal–ligand bond distances.<sup>18</sup>

Solid salts of the one-electron reduction product,  $[\text{Fe}(\text{CN})_5\text{NO}]^{3-}$ , have been obtained,<sup>39</sup> but no crystal structures are available. Table 1 shows that the reduction of  $[\text{Fe}(\text{CN})_5\text{NO}]^{2-}$  is associated with an overall increase in bond lengths, suggesting an increase of the electron population in the antibonding system, delocalized over the metal and the ligands. The increase is particularly noticeable for the Fe–N and N–O bond lengths, suggesting that most of the electronic density associated with the extra electron is localized in the  $\pi^*(\text{NO})$  orbital, which however could also contain some participation of Fe (see below). This is equivalent to consider that the  $[\text{Fe}(\text{CN})_5\text{NO}]^{3-}$  ion contains a partially reduced nitrosyl ligand. This description is consistent with the analysis of the frontier orbitals of both species. Whereas the LUMO is mainly centered in NO in  $[\text{Fe}(\text{CN})_5\text{NO}]^{2-}$  (Figure 2), the odd electron in the paramagnetic  $[\text{Fe}(\text{CN})_5\text{NO}]^{3-}$  complex is mainly localized on the N and O atoms, with spin Mulliken populations of 0.487 and 0.254, respectively, and a smaller contribution on Fe of 0.226. This agrees with both experimental<sup>40</sup> and previous DFT results obtained using partial optimizations performed within a discrete variational scheme.<sup>41</sup> In the  $[\text{Fe}(\text{CN})_5\text{NO}]^{n-}$  optimized structures, the calculated values of the Fe–N–O angles are 177.2° ( $n = 2$ ) and 146.6° ( $n = 3$ ). The first one agrees with the

(34) Pauncz, R. *Spin Eigenfunctions*; Plenum Press: New York, 1979.

(35) Chen, P.; Meyer, T. J. *Chem. Rev.* **1998**, *98*, 1439.

(36) Stavrev, K. K.; Zerner, M. C.; Meyer, T. J. *J. Am. Chem. Soc.* **1995**, *117*, 8684.

(37) Martin, C. H.; Zerner, M. C. In *Inorganic Electronic Structure and Spectroscopy*; Solomon, E. I., Lever, A. B. P., Eds.; John Wiley & Sons: New York, 1999.

(38) Carducci, M. D.; Pressprich, M. R.; Coppens, P. *J. Am. Chem. Soc.* **1997**, *119*, 2669.

(39) Nast, R.; Schmidt, J. *Angew. Chem., Int. Ed.* **1969**, *8*, 383.

(40) van Voorst, J. D.; Hemmerich, P. *J. Chem. Phys.* **1966**, *45*, 3914.

(41) Gómez, J. A.; Guenzburger, D. *Chem. Phys.* **2000**, *253*, 73.

**Table 2.** Calculated Selected Wavenumbers ( $\text{cm}^{-1}$ ) for  $[\text{Fe}(\text{CN})_5\text{NO}]^{2-}$  and Its Stable Reduction Products<sup>a</sup>

	C–N s	C–N s (exptl)	N–O s	N–O s (exptl)	Fe–N s
$[\text{Fe}(\text{CN})_5\text{NO}]^{2-}$	2156–2166	2156–2164 <sup>b</sup>	1932	1918 <sup>b</sup>	725
$[\text{Fe}(\text{CN})_5\text{NO}]^{3-}$	2000–2084	2075, 2095 <sup>c</sup>	1650	1568, 1608 <sup>c</sup>	657
$[\text{Fe}(\text{CN})_4\text{NO}]^{2-}$	2074–2107	2100 <sup>c</sup>	1782	1746 <sup>c</sup>	697
$[\text{Fe}(\text{CN})_4\text{NO}]^{3-}$	2010–2035		1581		657
$\text{Fe}(\text{CN})_5\text{NHO}]^{3-}$	1955–2018		1338–1394		808

<sup>a</sup> Experimental values are given for comparison. <sup>b</sup> Reference 46. <sup>c</sup> Reference 39.

experimental value for sodium nitroprusside<sup>38</sup> and with the linear conformations generally found for low-spin  $d^6$  nitrosyl complexes.<sup>42</sup> The bending in the reduced compound is typical of a  $\{\text{FeNO}\}^7$  system, named according to the Enemark–Feltham's notation.<sup>42</sup> A similar value,  $148^\circ$ , was found in the related  $[\text{Fe}^{\text{II}}(\text{NO})(\text{das})_2\text{Br}][\text{ClO}_4]$  compound (das = *o*-phenylenebis-(dimethylarsine)).<sup>43</sup> An angle of  $156^\circ$  was obtained for a complex of  $\text{FeEDTA-NO}$  with unknown structure, by performing EXAFS analysis studies, based on the angular dependence of multiple scattering effects;<sup>44a</sup> this value was consistent with those calculated for complexes in the  $\{\text{FeNO}\}^7$  series.<sup>44b</sup> The Fe–N and N–O distances obtained from the best fit for the  $\text{FeEDTA-NO}$  complex were 1.78 and 1.10 Å. Although the NO unit is an  $\text{NO}^-$  triplet spin-polarized with high-spin  $\text{Fe}^{\text{III}}$  in the EDTA complex, but NO bound to a low-spin  $\text{Fe}^{\text{II}}$  center in the  $[\text{Fe}(\text{CN})_5\text{NO}]^{3-}$  complex, there is bond distance similarity with the results shown in Table 1 for  $[\text{Fe}(\text{CN})_5\text{NO}]^{3-}$ .

The two-electron reduced species,  $[\text{Fe}(\text{CN})_5\text{NO}]^{4-}$ , has not been described in the literature. Our calculations showed it to be unstable in vacuo. A stable species was however predicted upon protonation of the N atom (see below).

**Spectroscopic Characterization of Stable Pentacyanide Species.** Table 2 shows some selected IR wavenumbers, as obtained by DFT calculations for the species that we calculate as stable. The values for  $[\text{Fe}(\text{CN})_5\text{NO}]^{2-}$  agree with a vibrational analysis performed previously using DFT tools.<sup>45</sup> At the LDA level, the values for  $\nu_{\text{CN}}$  (ca.  $2160 \text{ cm}^{-1}$ ) and  $\nu_{\text{NO}}$  ( $1932 \text{ cm}^{-1}$ ) are in agreement with experiment<sup>46</sup> and consistent with the formal consideration of the nitrosyl ligand as a  $\text{NO}^+$  species.

Additional structural confirmation is given by the UV–vis calculated bands. We center the discussion in the low energy bands, which are the most strongly sensitive to structure. Table 3 allows the comparison of the results of our calculations with the experimental data previously reported by Manoharan and Gray.<sup>47a</sup> In agreement with experiment, we found two bands in the visible and one in the UV region. The difference between the experimental and calculated data is, in all cases, within the error expected for this methodology.<sup>37</sup> It is larger for the high energy bands, an effect usually found in these calculations, which is mainly attributed to the fact that double excitations are not included. The calculated and experimental intensities give the same trend of variation, and even their relative values can be compared. The bands in the visible are assigned to MLCT  $\text{Fe}^{\text{II}} \rightarrow \pi^*(\text{NO}^+)$  transitions, whereas the band in the UV to a

**Table 3.** UV–Vis Spectroscopic Features of the Compounds Calculated as Stable<sup>a</sup>

$E(\text{calc})$ ( $\text{cm}^{-1}$ )	oscillator strength	$E(\text{exp})^c$ ( $\text{cm}^{-1}$ )	assignment	
20847	0.00004	20000 (4) <sup>b</sup>	CT Fe $\rightarrow$ NO	$[\text{Fe}(\text{CN})_5\text{NO}]^{2-}$
23180	0.00014	25300 (8) <sup>b</sup>	CT Fe $\rightarrow$ NO	
23712	0.00059			
29189	0.00050	30300 (50) <sup>b</sup>	LF	
29379	0.00152			
21288	0.00138	23180 (550) <sup>d</sup>	LF	$\text{Fe}(\text{CN})_5\text{NO}]^{3-}$
21382	0.00340			
28427	0.01000	28985 (3500) <sup>d</sup>	CT Fe $\rightarrow$ NO	
18800	0.0001		LF	$\text{Fe}(\text{CN})_5\text{HNO}]^{3-}$
19300	0.0001		LF	
21770	0.0010		CT Fe $\rightarrow$ NO	
29552	0.0050		LF	
30128	0.2700		CT Fe $\rightarrow$ NO	
15342	0.0056	16200 (380) <sup>d</sup>	LF	$[\text{Fe}(\text{CN})_4\text{NO}]^{2-}$
15752	0.0059			
23702	0.0021	23256 (100) <sup>d</sup>	CT Fe $\rightarrow$ NO	
27133	0.0016	28570 (300) <sup>d</sup>	LF	
13763	0.0002		LF	$[\text{Fe}(\text{CN})_4\text{NO}]^{3-}$
15907	0.0010		CT Fe $\rightarrow$ NO	
20580	0.0020		LF	

<sup>a</sup> Experimental values are reported, for comparison, whenever available. <sup>b</sup> Intensity between brackets ( $\epsilon$ ). <sup>c</sup> Reference 47. <sup>d</sup> Reference 54.

LF excitation. This assignment for the first two bands has been claimed to be correct several times, according to CNDO calculations,<sup>48</sup> ESR,<sup>48</sup> XPS,<sup>49</sup> optical electronic spectra in solution and with polarized light in crystals,<sup>47b</sup> and Mössbauer spectroscopy.<sup>50</sup> The influence of the solvent was modeled, in this case, by means of five point charges of  $+0.4e$ , located at 1.4 Å of each  $\text{CN}^-$  ligand. The system thus defined bears no charge as a whole. Within this scheme, working with the nonsymmetrized DFT optimized geometry, no degeneracy results in the calculated ZINDO/S MO distribution. The two highest occupied MO are, however, almost degenerate and  $d$  in nature. The LUMO and LUMO + 1 are also almost degenerate and described as  $\pi^*(\text{NO})$ . This MO description, which is in close agreement with the one previously derived by Manoharan and Gray on the basis of extended Hückel (EH) calculations,<sup>47</sup> is not attained when the solvent is not modeled. In this case, the HOMOs have a large contribution of the CN orbitals, which mix with the Fe ones. NO orbitals also mix with those of Fe to define the LUMOs. This description resembles several ones previously given, which have been obtained by means of different methodologies with no consideration of the solvent<sup>51–53</sup> and also with the DFT calculations performed in this work for isolated  $[\text{Fe}(\text{CN})_5\text{NO}]^{2-}$ . In this way, lack of modeling

(42) Feltham, R. D.; Enemark, J. H. *Topics Inorg. Organomet. Stereochem.* **1981**, 12, 155.

(43) Quinby Hunt, M.; Feltham, R. D. *Inorg. Chem.* **1978**, 17, 2515.

(44) (a) Zhang, Y.; Pavlosky, M. A.; Brown, C. A.; Westre, T. E.; Hedman, B.; Hodgson, K. O.; Solomon, E. I. *J. Am. Chem. Soc.* **1992**, 114, 9189. (b) Westre, T. E.; Di Cicco, A.; Filipponi, A.; Natoli, C. R.; Hedman, B.; Solomon, E. I.; Hodgson, K. O. *J. Am. Chem. Soc.* **1994**, 116, 6757.

(45) Estrin, D. A.; Baraldo, L. M.; Slep, L. D.; Barja, B. C.; Olabe, J. A. *Inorg. Chem.* **1996**, 35, 3897.

(46) Paliani, G.; Poletti, A.; Santucci, A. J. *Mol. Struct.* **1971**, 8, 63.

(47) (a) Manoharan, P. T.; Gray, H. B. *J. Am. Chem. Soc.* **1965**, 87, 3340. (b) Manoharan, P. T.; Gray, H. B. *Inorg. Chem.* **1966**, 5, 823.

(48) Fenske, R. F.; DeKock, R. L. *Inorg. Chem.* **1972**, 11, 437.

(49) Calabrese, A.; Hayes, R. G. *J. Am. Chem. Soc.* **1974**, 96, 5054.

(50) (a) Hauser, U.; Oestreich, V.; Rohrweck, H. D. *Z. Phys.* **1977**, A280, 17; **1978**, A284, 9. (b) Braga, M.; Pavao, A. C.; Leite, J. R. *Phys. Rev. B* **1981**, 23, 4328.

(51) Hollauer, E.; Olabe, J. A. *J. Braz. Chem. Soc.* **1997**, 8(5), 495.

(52) Bottomley, F.; Grein, F. *J. Chem. Soc., Dalton Trans.* **1980**, 1359.

(53) (a) Golebiewski, A.; Wasielewska, E. *J. Mol. Struct.* **1980**, 67, 183. (b) Wasielewska, E. *Inorg. Chim. Acta* **1986**, 113, 115.

the solvent seems to be the origin of the controversy among the related data. The calculations by Fenske and DeKock,<sup>48</sup> whose results agree with ours, support this inference, as they have applied an eigenvalue shifting as a way of incorporating the influence of the environment.

Upon one-electron reduction of  $[\text{Fe}(\text{CN})_5\text{NO}]^{2-}$  in aqueous solution, a pH-dependent mixture of a brown and a blue species is obtained.<sup>9,40</sup> It has been proposed that the brown one (predominant at pH's around 9) corresponds to the  $[\text{Fe}(\text{CN})_5\text{NO}]^{3-}$  ion, while the blue one,  $[\text{Fe}(\text{CN})_4\text{NO}]^{2-}$ , appears as a result of cyanide release, this being favored by low pHs (see eq 1).<sup>54</sup> As shown below, our calculations confirm that not only  $[\text{Fe}(\text{CN})_5\text{NO}]^{3-}$  but also  $[\text{Fe}(\text{CN})_4\text{NO}]^{3-}$  are stable species in equilibrium. For  $[\text{Fe}(\text{CN})_5\text{NO}]^{3-}$ , the predicted  $\nu_{\text{CN}}$  are in the range 2000–2084  $\text{cm}^{-1}$ , while  $\nu_{\text{NO}}$  appears at 1650  $\text{cm}^{-1}$ . The C–N and N–O stretchings agree fairly well with experimental values found for some salts of  $[\text{Fe}(\text{CN})_5\text{NO}]^{3-}$  (2075–2095 for  $\nu_{\text{CN}}$ , 1568–1608 for  $\nu_{\text{NO}}$ ).<sup>39</sup> The sharp decrease of  $\nu_{\text{NO}}$  upon reduction is another evidence of the major localization of the additional electron at the NO ligand, as has been also found for the ruthenium and osmium pentacyanide analogues<sup>55</sup> and confirmed by our estimation of the spin Mulliken populations.

The calculated electronic spectrum for  $[\text{Fe}(\text{CN})_5\text{NO}]^{3-}$  predicts a LF band at 470 nm, together with a MLCT band at 347 nm, of higher intensity. According to Table 3, there is good agreement with the experimental data reported in ref 54. The calculated intensities are larger than for the nitroprusside ion, showing also the proper trend of variation. The solvent has been modeled, in this case, by means of five point charges of +0.6e, located at 1.0 Å of each CN ligand, giving, as before, a neutral system. The MO description is similar to the one previously given for the  $[\text{Fe}(\text{CN})_5\text{NO}]^{2-}$  complex, with the odd electron occupying a  $\pi^*(\text{NO})$  orbital. This description is in agreement, on the other hand, with the one derived from DFT calculations.

In contrast to the unstable  $[\text{Fe}(\text{CN})_5\text{NO}]^{4-}$  ion, the calculations show that a stable two-electron-reduced species is obtained upon protonation of the N-atom, as detailed below. This important but very elusive species has not been properly characterized yet, although there is strong evidence for it being an intermediate in different processes. The stabilization of the so-called “nitroxyl” species,  $\text{NO}^-$ , upon coordination and protonation was shown for some complexes closely related to  $[\text{Fe}(\text{CN})_5\text{HNO}]^{3-}$ , namely  $[\text{Ru}^{\text{II}}(\text{hedta})(\text{NO})]^{2-}$ ,  $[\text{Re}^{\text{I}}(\text{CO})_3(\text{PPh}_3)_2(\text{HNO})]^+$ , and  $[\text{Os}^{\text{II}}\text{Cl}_2(\text{CO})(\text{HNO})(\text{PPh}_3)_2]$ .<sup>8,56,57</sup> The calculated IR spectrum of  $[\text{Fe}(\text{CN})_5\text{HNO}]^{3-}$  shows a strong band at 2983  $\text{cm}^{-1}$  ( $\nu_{\text{N-H}}$ ), two bands at 1394 and 1338  $\text{cm}^{-1}$  corresponding to  $\nu_{\text{NO}}$  modes with some H participation, and bands assigned to  $\nu_{\text{CN}}$  in a range from 1955 to 2018  $\text{cm}^{-1}$ . The N–O stretchings are consistent with the values found for the above-mentioned complexes: 1383, 1391, and 1410  $\text{cm}^{-1}$ , respectively. The  $\nu_{\text{CN}}$  values agree with those found for cyanides bound to Fe(II) complexes bearing other weak-to-moderate  $\pi$ -acceptor ligands.<sup>58</sup> The very low value for  $\nu_{\text{NO}}$  reveals that the second electron enters also the antibonding orbital mainly centered on the nitrosyl moiety. This is consistent with the calculated very large NO bond distance (see below). The UV–

**Table 4.** Free Energy Changes (kcal/mol) Associated to the Process:  $[\text{Fe}(\text{CN})_5\text{NO}]^{3-} \rightarrow [\text{Fe}(\text{CN})_4\text{NO}]^{2-} + \text{CN}^-$

LDA	GGA	GGA(water)	GGA(acetonitrile)	exp (water) <sup>a</sup>
–90.6	–101.3	8.4	3.9	5.7

<sup>a</sup> Reference 54.

**Table 5.** Selected Structural Parameters (Å and deg) for the  $[\text{Fe}(\text{CN})_4\text{NO}]^{n-}$  Anions ( $n = 2, 3$ )

	$n = 2$ (exp) <sup>a</sup>	$n = 2$	$n = 3$
$r(\text{FeC}1)$	1.887	1.864	1.863
$r(\text{FeC}2)$	1.897	1.885	1.893
$r(\text{FeC}3)$	1.887	1.885	1.884
$r(\text{FeC}4)$	1.897	1.885	1.907
$r(\text{FeN}5)$	1.565	1.625	1.637
$r(\text{C}1\text{N}1)$	1.154	1.181	1.191
$r(\text{C}2\text{N}2)$	1.164	1.18	1.189
$r(\text{C}3\text{N}3)$	1.154	1.18	1.188
$r(\text{C}4\text{N}4)$	1.164	1.178	1.188
$r(\text{N}5\text{O})$	1.161	1.184	1.22
$\angle\text{FeN}5\text{O}$	177.1	171.4	171.2
$\angle\text{C}2\text{FeC}1$	85.7	86.1	107.1
$\angle\text{N}5\text{FeC}1$	102.3	101.2	117.9

<sup>a</sup> Ref 60. No standard deviations have been reported.

vis spectrum, computed using five point charges of 0.6e at 1.4 Å of each cyanide ligand, is characterized by an intense feature at 330 nm, together with bands of lower intensity at 450 nm, both assigned to MLCT excitations. This description is in qualitative agreement with the spectra determined after electrolysis of the nitroprusside ion under conditions of 2-electron reduction, which show a band at 345 nm, together with one of lower intensity at 445 nm. There are also bands at 240 nm in the experimental spectra,<sup>7</sup> which we calculate and assign to MLCT transitions involving the CN ligands.

**Cyanide Release Reactions: The  $[\text{Fe}(\text{CN})_4\text{NO}]^{n-}$  Species ( $n = 2, 3$ ).** It has been reported that the one-electron reduced species derived from  $[\text{Fe}(\text{CN})_5\text{NO}]^{2-}$  releases cyanide according to eq 1:<sup>9,54</sup>



The free energy change for reaction 1 is given in Table 4, as it results from calculations in vacuo and in aqueous solution. Due to the fact that both reactants and products are charged species, solvent effects have a sizable influence in the computed values. Reaction 1 turns out to be slightly endergonic in aqueous solution; the computed  $\Delta G^\circ$  value of 8.4 kcal/mol agrees reasonably well with the experimental value of 5.7 kcal/mol.<sup>54</sup> Remarkably, the process is predicted to be spontaneous in vacuo, while  $\Delta G^\circ$  is expected to decrease when going from water to less polar solvents. In fact, computations in acetonitrile predict a value of 3.9 kcal/mol. This is consistent with the fact that  $[\text{Fe}(\text{CN})_5\text{NO}]^{3-}$  decomposes completely in organic solvents according to reaction 1.<sup>59</sup>

The product of reaction 1, the  $[\text{Fe}(\text{CN})_4\text{NO}]^{2-}$  ion, has been well characterized as a tetrabutylammonium salt.<sup>60</sup> The anion displays a distorted square-pyramidal structure, and spectroscopic characterization data are available. The data that result from a geometry optimization of  $[\text{Fe}(\text{CN})_4\text{NO}]^{2-}$  (Table 5, Figure 3) agree reasonably well with the experimental X-ray results. The experimental<sup>39</sup> and DFT predicted values for  $\nu_{\text{CN}}$

(54) Cheney, R. P.; Simic, M. G.; Hoffman, M. Z.; Taub, I. A.; Asmus, K. D. *Inorg. Chem.* **1977**, *16*, 2187.

(55) (a) Baumann, F.; Kaim, W.; Baraldo, L. M.; Slep, L. D.; Olabe, J. A.; Fiedler, J. *Inorg. Chim. Acta* **1999**, *285*, 129. (b) Kaim, W.; Olabe, J. A. Unpublished work.

(56) Southern, J. S.; Hillhouse, G. L. *J. Am. Chem. Soc.* **1997**, *119*, 12406.

(57) (a) Grundy, K. R.; Reed, C. A.; Roper, W. R. *J. Chem. Soc., Chem. Commun.* **1970**, 1501. (b) Wilson, R. D.; Ibers, J. A. *Inorg. Chem.* **1979**, *18*, 336.

(58) Toma, H. E.; Malin, J. M. *Inorg. Chem.* **1973**, *12*, 1039.

(59) Bowden, W. L.; Bonnar, P.; Brown, D. B.; Geiger, W. E. *Inorg. Chem.* **1977**, *16*, 41.

(60) Schmidt, J.; Kuhr H.; Dorn, W. L.; Kopf, J. *Inorg. Nucl. Chem. Lett.* **1974**, *10*, 55.

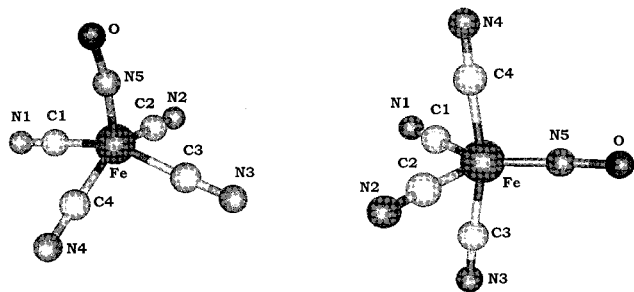


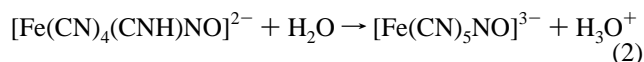
**Figure 3.** Optimized structures of  $[\text{Fe}(\text{CN})_4\text{NO}]^{2-}$  and  $[\text{Fe}(\text{CN})_4\text{NO}]^{3-}$  ions.

and  $\nu_{\text{NO}}$ , (Table 2) show good agreement. It has been suggested that the  $[\text{Fe}(\text{CN})_4\text{NO}]^{2-}$  ion contains Fe in oxidation state +1, with  $\text{NO}^+$  as a ligand.<sup>10</sup> We calculate that the odd electron in the latter complex is mainly localized at the iron atom, with a spin Mulliken population of 0.920e. This agrees with ESR<sup>40,61</sup> and IR measurements,<sup>39</sup> as well as with previous DFT calculations.<sup>41</sup>

The calculated UV–vis spectrum of  $[\text{Fe}(\text{CN})_4\text{NO}]^{2-}$  gives an intense band at 645 nm, associated with a LF transition, together with bands of lower intensity at 422 and 368 nm, assigned to MLCT and LF transitions, respectively. The comparison with the experimental data (Table 3) demonstrates the accuracy of the calculations. Solvent simulation was based on the definition of four point charges of +0.5 at 1.0 Å of each CN ligand.

A more reduced species has been obtained electrochemically from  $[\text{Fe}(\text{CN})_4\text{NO}]^{2-}$  and described as  $[\text{Fe}(\text{CN})_4\text{NO}]^{3-}$ .<sup>7,61</sup> Although it has not been properly characterized, our optimization procedure suggests that it is a stable species with a trigonal bipyramidal structure (Figure 3). The structural parameters of  $[\text{Fe}(\text{CN})_4\text{NO}]^{3-}$  are given in Table 5. It can be noted that the CN, and particularly the NO bond distances, are larger in the more reduced species (compare  $[\text{Fe}(\text{CN})_4\text{NO}]^{3-}$  to  $[\text{Fe}(\text{CN})_4\text{NO}]^{2-}$ ). The computed IR spectrum of the  $[\text{Fe}(\text{CN})_4\text{NO}]^{3-}$  complex shows an expected decrease for  $\nu_{\text{CN}}$  and  $\nu_{\text{NO}}$ , compared to the values obtained for  $[\text{Fe}(\text{CN})_4\text{NO}]^{2-}$  (Table 2). There are no experimental data to compare with the calculated UV–vis spectrum, shown in Table 3. The distribution of point charges (+0.75 at 1.6 of each CN ligand) in the model used for these calculations is consistent with the absence of negative charge on the NO ligand.

**Acid–Base Reactions. Protonation of Cyanide or Nitrosyl Ligands.** It is known that the  $[\text{Fe}(\text{CN})_5\text{L}]^{n-}$  complexes, with L being a  $\sigma$ -only ligand (like  $\text{H}_2\text{O}$  or  $\text{NH}_3$ ) or any weak-to-moderate  $\pi$ -acceptor ligand, can protonate at the cyanide ligands in the pH range 0–3, depending on  $L$ .<sup>58</sup> This is not the case for the strongly acceptor  $\text{NO}^+$ , but it is feasible that the NO-reduced species could also protonate. We have optimized the structures of all possible protonated complexes that may result from one- and two-electron reduction of  $[\text{Fe}(\text{CN})_5\text{NO}]^{2-}$ . Protonation on equatorial and axial cyanides and on the N and O atoms of NO have been considered. The relative stabilities of all the structures are given in Table 6. For  $[\text{Fe}(\text{CN})_5\text{NO}]^{3-}$ , it turns out that the protonation of the cyanides, either in equatorial or axial positions, is favored over the protonation of the NO. Thus, the  $\Delta G^\circ$  for reaction 2



was predicted to be 8.6 and 11.2 kcal/mol, for the axial and equatorial protonated species, respectively. The stabilization of

**Table 6.** Relative Energies (kcal/mol) of Different Protonated Derivatives of the  $[\text{Fe}(\text{CN})_5\text{NO}]^{n-}$  Anion ( $n = 3, 4$ )

protonation site	$[\text{Fe}(\text{CN})_5\text{NO}]^{3-}$		$[\text{Fe}(\text{CN})_5\text{NO}]^{4-}$	
	GGA	GGA–PCM	GGA	GGA–PCM
CN(ax)	1.2	2.6	26.0	25.6
CN(eq)	0.0	0.0	22.4	24.4
O(NO)	32.0	28.7	23.9	20.6
N(NO)	6.8	19.9	0.0	0.0

**Table 7.** Selected Structural Parameters (Å and Deg) for the  $[\text{Fe}(\text{CN})_4(\text{CNH})\text{NO}]^{2-}$  and  $[\text{Fe}(\text{CN})_5\text{NHO}]^{3-}$  Anions, as They Result from DFT Calculations

	$[\text{Fe}(\text{CN})_4(\text{CNH})\text{NO}]^{2-}$		$[\text{Fe}(\text{CN})_5\text{NHO}]^{3-}$
	CN ax	CNeq	
$r(\text{FeC1})$	1.911	1.737	1.902
$r(\text{FeC2})$	1.902	1.913	1.909
$r(\text{FeC3})$	1.900	1.923	1.911
$r(\text{FeC4})$	1.903	1.900	1.907
$r(\text{FeC5})$	1.745	1.898	1.915
$r(\text{FeN6})$	1.769	1.752	1.783
$r(\text{C1N1})$	1.18	1.215	1.183
$r(\text{C2N2})$	1.176	1.178	1.184
$r(\text{C3N3})$	1.179	1.177	1.182
$r(\text{C4N4})$	1.181	1.177	1.182
$r(\text{C5N5})$	1.213	1.177	1.179
$r(\text{N6O})$	1.184	1.193	1.249
$r(\text{N1H})$		1.034	
$r(\text{N5H})$	1.034		
$r(\text{N6H})$			1.056
(FeN6O)	143.3	140.1	137.5
(HN5C5)	126.8		
(HN1C1)		123.2	
(HN6Fe)			110.5
(HN6O)			110.5

the negative charge in the protonated cyanide is probably responsible for the large increase in the CN bond length relative to the nonprotonated cyanides. This is also consistent with the effect observed in the HNC bond angles, which are close to those corresponding to an  $\text{sp}^2$  hybridization, and implies, then, a double CN bond, instead of the triple bond characteristic of nonprotonated cyanides. On the other hand, the two-electron reduction product protonates preferentially on the NO nitrogen atom.

As described above, the stable two-electron reduction product of  $[\text{Fe}(\text{CN})_5\text{NO}]^{2-}$  was proposed to be the protonated  $[\text{Fe}(\text{CN})_5\text{HNO}]^{3-}$  ion (Figure 4), a species that is predicted to form spontaneously in water. Table 7 shows some selected geometrical parameters for this species. When the structural data of the two-electron reduced  $[\text{Fe}(\text{CN})_5\text{HNO}]^{3-}$  complex are compared with those of the one-electron reduced  $[\text{Fe}(\text{CN})_5\text{NO}]^{3-}$  ion (Table 1), the larger value of the NO bond distance, as well as the larger bending of the Fe–N–O bond ( $137.5^\circ$ ) in the two-electron reduced product, appear as remarkable; the angle value is close to the one reported for  $[\text{Os}^{\text{II}}\text{Cl}_2(\text{CO})(\text{HNO})(\text{PPh}_3)_2]$ ,  $136.9^\circ$ .<sup>57b</sup> This adds strong evidence on the presence of a “nitroxyl” species (see above the analysis of spectroscopic calculations, which also were found to be consistent with the results obtained experimentally for complexes in which the bound HNO ligand has been well characterized).<sup>56,57</sup> Although direct spectroscopic evidence on the  $[\text{Fe}(\text{CN})_5\text{HNO}]^{3-}$  ion is unavailable; the stable product of the two-electron electrochemical reduction of the nitroprusside ion (see above) has been tentatively described as  $[\text{Fe}(\text{CN})_4(\text{NC})\text{NO}]^{4-}$ ;<sup>7</sup> the reported spectrum is close to the one presently calculated for  $[\text{Fe}(\text{CN})_5\text{HNO}]^{3-}$ . In the reaction of  $[\text{Fe}(\text{CN})_5\text{NO}]^{2-}$  with  $\text{NH}_2\text{OH}$ , the

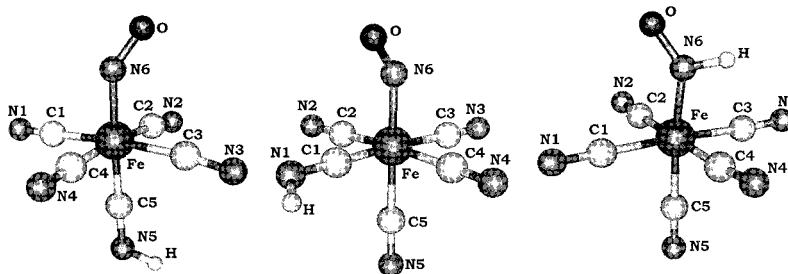


**Figure 4.** Optimized structures of the most stable protonated complexes of  $[\text{Fe}(\text{CN})_5\text{NO}]^{3-}$  and  $[\text{Fe}(\text{CN})_5\text{NO}]^{4-}$ .

$[\text{Fe}(\text{CN})_5\text{HNO}]^{3-}$  ion could be a reactive intermediate in the route to  $\text{N}_2\text{O}$  formation.<sup>62</sup>

### Conclusions

The bond lengths and angles resulting from the geometry optimization of the nitroprusside ion (bearing a formal  $\text{NO}^+$ -bound species) are in good agreement with structural X-ray results. Infrared and UV-vis spectra can be also successfully interpreted by means of DFT and ZINDO/S calculations, respectively.

Although no single-crystal structure is available, the geometry optimization and spectroscopic predictions for the one-electron reduced compound,  $[\text{Fe}(\text{CN})_5\text{NO}]^{3-}$ , are also consistent with the available experimental results and confirm the inference that the extra-electron occupies a delocalized molecular orbital mainly centered on the NO ligand. According to the calculations, the  $[\text{Fe}(\text{CN})_5\text{NO}]^{3-}$  ion affords protonation on cyanides but not on the NO ligand. This endergonic process could occur significantly at low pHs.

The two-electron reduction product,  $[\text{Fe}(\text{CN})_5\text{NO}]^{4-}$ , is calculated as unstable, but the species protonated at the N atom of NO,  $[\text{Fe}(\text{CN})_5\text{HNO}]^{3-}$ , turns out to be stable. The geometry optimization and spectral calculations (particularly the structural and IR predictions associated to the Fe-N-O moiety) are in good agreement with the values that can be expected for protonated "nitrosyl" species, as those found in related complexes of Ru(II), Re(I), and Os(II), which bear the same low-spin  $d^6$  configurations as Fe(II). Although the  $[\text{Fe}(\text{CN})_5\text{HNO}]^{3-}$  ion has not been fully characterized, the spectroelectrochemical generation of a species probably containing bound  $\text{NO}^-$  has been reported in the literature; many evidences point to  $[\text{Fe}(\text{CN})_5\text{HNO}]^{3-}$  as a reactive intermediate in the redox interconversions of nitrite and nitrogen hydrides on iron-pentacyanide centers, as well as a precursor of  $\text{N}_2\text{O}$  formation.

DFT and ZINDO/S methodologies also became useful in the calculation of structural and spectroscopic parameters for the tetracyano-species,  $[\text{Fe}(\text{CN})_4\text{NO}]^{n-}$ , ( $n = 2, 3$ ), which are formed through cyanide release from the pentacyano-ones upon one- or two-electron reduction processes.

(62) (a) Wolfe, S. K.; Andrade, C.; Swinehart, J. H. *Inorg. Chem.* **1974**, *13*, 2567. (b) Banyai, I.; Dozsa, L.; Beck, M. T.; Gyemant, G. *J. Coord. Chem.* **1996**, *37*, 257. (c) Alluisetti, G.; Amorebieta, V. T.; Olabe, J. A. Manuscript in preparation. The decomposition of hydroxylamine is catalyzed by pentacyano(L)ferrate(II) ions. The products are  $\text{NH}_3$  and  $\text{N}_2\text{O}$  (and also  $\text{N}_2$ , depending on conditions), and some  $[\text{Fe}(\text{CN})_5\text{NO}]^{2-}$  can also be formed. It is proposed that disproportionation occurs through two-electron changes, by attack of free  $\text{NH}_2\text{-OH}$  on the  $[\text{Fe}(\text{CN})_5\text{NH}_2\text{OH}]^{3-}$  ion. In this context, the  $[\text{Fe}(\text{CN})_5\text{HNO}]^{3-}$  could be a necessary precursor for  $\text{N}_2\text{O}$  formation.

**Acknowledgment.** This work was partially supported by the Fundación Antorchas and the University of Buenos Aires. D.A.E., G.E., and J.A.O. are members of the scientific staff, and D.A.S. is a doctoral fellow of CONICET (National Scientific Council, Argentina).

IC010140P